A Journal of the Gesellschaft Deutscher Chemiker

Angewandte International Edition Chemie

GDCh

www.angewandte.org

Accepted Article

Title: Environmental-Friendly Solid Synthesis of Fe-N-C Electrocatalyst with Fe Exclusively in Atomically Dispersed Fe-N4 Moieties for High-Power Proton Exchange Membrane Fuel Cells

Authors: Qingtao Liu, Xiaofang Liu, Lirong Zheng, and Jianglan Shui

To be cited as: *Angew. Chem. Int. Ed.* 10.1002/anie.201709597
Angew. Chem. 10.1002/ange.201709597

Link to VoR: http://dx.doi.org/10.1002/anie.201709597
http://dx.doi.org/10.1002/ange.201709597

WILEY-VCH

10.1002/anie.201709597

WILEY-VCH

Environmental-Friendly Solid Synthesis of Fe-N-C Electrocatalyst with Fe Exclusively in Atomically Dispersed Fe-N_4 Moieties for High-Power Proton Exchange Membrane Fuel Cells

Qingtao Liu,[a] Xiaofang Liu,*[a] Lirong Zheng,[b] and Jianglan Shui*[a]

Abstract: Environmental-friendly synthesis of highly active Fe-N-C electrocatalyst for proton exchange membrane fuel cells (PEMFCs) is desirable but remains challenging. Herein, we report a green, simple and scalable method to fabricate Fe(II)-doped ZIF-8, which can be further pyrolyzed into Fe-N-C with 3 wt.% of Fe exclusively in Fe-N_4 active moieties. Significantly, this Fe-N-C derived acidic PEMFC exhibits an unprecedented current density of 1.65 A cm^{-2} at 0.6 V and the highest power density of 1.14 W cm^{-2} compared with previously reported NPMCs. The excellent PEMFC performance can be attributed to the densely and atomically dispersed Fe-N_4 active moieties on the small and uniform catalyst nanoparticles.

Proton exchange membrane fuel cells (PEMFCs) are ideal clean energy systems that efficiently convert chemical energy of hydrogen/oxygen to electricity through electrochemical reactions.[1] The application of PEMFCs is, however, hindered by the scarcity and intolerable cost of precious metal Pt which is the most efficient catalyst so far for oxygen reduction reaction (ORR), and accounts for ~40% of the fuel cell cost.[2] As a non-precious metal catalyst (NPMC), Fe-N-C decorated with Fe-N_4 active moieties has emerged as a promising alternative to Pt for its high initial performance close to commercial Pt/C(20%) in acidic PEMFCs.[3] The maximum power densities (P_{max}) of these Fe-N-C derived PEMFCs have reached above 0.9 W cm^{-2} or even over 1 W cm^{-2} to date (the largest P_{max} of 1.06 W cm^{-2} achieved at 2 bar H_2/O_2@80 °C in 2017).[4]

Although the three-electrode system (half-cell) is efficient for a fast judgement of the NPMC catalytic activity, PEMFC measurement is more valuable for comprehensively evaluating catalyst properties in the actual working condition.[5] The NPMC fuel cell performance is commonly determined by two factors. One is the mass transport property of the catalyst layer, which influences the utilization of the active sites and the polarization of the fuel cell;[6] the other is the catalyst parameters, including the composition and the dispersion density of active sites, and the catalyst morphology and size which in turn affect the first factor.[4b, 7] Due to the lower activity, Fe-N-C catalyst layers (CLs) are usually much thicker than Pt/C layers in PEMFCs, which results in higher internal resistances and consequently more serious polarization, faster current drop and smaller P_{max}. So far, the effects of Fe-N-C morphology, size and active-site distribution on the PEMFC current and power densities have not been clearly identified, and the fuel cell performance still needs to be improved to promote their practical application.

The Fe-N-C parameters depend on the synthesis process, which typically involves a mixing of carbon, nitrogen and iron precursors, plus an annealing to obtain Fe-N_x active moiety doped porous carbon.[8] Impurities of Fe/Fe_3C nanoparticles (NPs) are usually formed due to the agglomeration of Fe atoms, leading to a low utilization of Fe precursors and a low dispersion density of Fe-N_x moieties.[9] Although an intense acid wash can remove Fe/Fe_3C NPs, it readily corrodes the active sites as well and changes the composition of as-annealed Fe-N-C.[4b, 8c, 10] To enhance the catalytic activity, an ammonia post-treatment is commonly applied to introduce more N-dopants into Fe-N-C.[4a, 8b, 11] Besides, considerable amounts of solvents (e.g. alcohol and organic solvents)[4a, b, 5a, 8b] and assistant reagents (e.g. surfactants)[12] are often used for precursor preparation, thus producing numerous waste. No matter solvents/assistant reagents or ammonia/acids, they increase environmental burden and fabrication cost, which would be serious problems for the mass production of Fe-N-C. Therefore, it is necessary to develop a green, low-cost, facile and scalable method to fabricate high quality Fe-N-C catalyst with favorable morphology and less Fe impurities, to meet the application needs in future.

Herein, Fe(II)-doped zeolitic imidazolate frameworks (ZIF-8) were successfully prepared, for the first time, by a one-step solid synthesis with no assistant reagents/solvents or waste. After a pyrolysis under Ar atmosphere, iron(II) ions were exclusively converted into atomically dispersed Fe-N_4 moieties in the final catalyst (3 wt.% Fe) with no needs of post-acid or -ammonia treatments. In a 5 cm^2 PEMFC, our Fe-N-C catalyst achieved unprecedentedly high power densities of 1.14 and 1.11 W cm^{-2} with 2.5 and 2.0 bar H_2/O_2, respectively. The highest current densities of 0.31 and 1.65 A cm^{-2} were also recorded at 0.8 and 0.6 V, respectively.

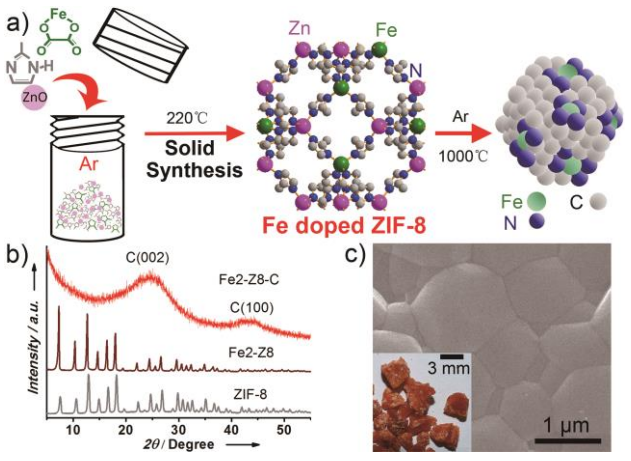

Figure 1. a) Scheme of the solid synthesis of Fe-doped-ZIF-8 crystal and carbonization for final Fe-N-C catalyst, b) XRD patterns of ZIF-8, Fe2-Z8 and Fe2-Z8-C, c) SEM image of Fe2-Z8 (Inset: photo image).

[a] Q. Liu, Assoc. Prof. X. Liu, Prof. J. Shui
School of Materials Science and Engineering
Beihang University
No. 37 Xueyuan Road, Beijing 100083, China
E-mail: liux05@buaa.edu.cn; shuijianglan@buaa.edu.cn
[b] Dr. L. Zheng
Beijing Synchrotron Radiation Facility, Institute of High Energy Physics, Chinese Academy of Sciences
No. 19 Yuquan Road, Beijing 100049, China

Supporting information for this article is given via a link at the end of the document.

The solid synthesis of Fe-N-C catalyst is illustrated in Figure 1a. Firstly, a powder mixture of 2-methylimidazole (2MIm), ZnO and ferrous oxalate ($FeC_2O_4 \cdot 2H_2O$, FeOx) was sealed in an autoclave under argon, and heated at 220 °C to form Fe(II)-doped ZIF-8 crystals by a one-step solvent-free process. 2MIm was melted at 220 °C ensuring a well contact with ZnO and a homogeneous crystallization. FeOx decomposed simultaneously releasing Fe^{2+} to partially replace Zn^{2+}, producing the coordinated Fe-N_4 in the doped ZIF-8 crystal. The molar percentage of Fe (in all metal ions) was 2 at.%, and the corresponding doped ZIF-8 was denoted as Fe2-Z8. Importantly, no waste or by-product was produced during the solid synthesis of Fe2-Z8. The identical XRD diffraction pattern of Fe2-Z8 to that of ZIF-8 indicates the successful incorporation of Fe^{2+} into ZIF-8 framework (Figure 1b). Meanwhile, the Fe^{2+} doping enhanced the crystallinity of Fe2-Z8 and darkened its color compared with the white ZIF-8 powder as observed by scanning electronic microscopy (SEM) and photo image in Figure 1c (ZIF-8 morphology was supplied below). The synthesis of Fe2-Z8 could be easily scaled up because no liquid was used and therefore the required reaction space was small (e.g. a 50 ml autoclave for tens of grams of products in one batch) (Figure S1). It implies that our method is particularly suitable for mass production. Subsequently, the large Fe2-Z8 crystals were ball-milled into powder, and washed quickly in a dilute polyvinyl pyrrolidone (PVP) solution to coat a molecular layer of PVP on Fe2-Z8 which prevented the individual particles from merging together during the annealing. It is noteworthy that the PVP solution did not produce detectable waste because the dilute PVP solution could be circularly utilized by adding new PVP powder. The PVP-coated Fe2-Z8 was then carbonized at 1000 °C in Ar to obtain the final Fe2-Z8-C electrocatalyst without any further treatment. Owing to the existence of immediately available nitrogen atoms and the firm bonding of Fe-N coordination to the neighboring carbon atoms of the whole framework, Fe atoms were isolated and converted into densely dispersed Fe-N_4 active moieties without aggregation into Fe NPs, as proved by the XRD (Figure 1b) and the following images and spectra results. As no assistant reagent was used in preparing Fe2-Z8, and neither ammonia nor acid treatment was applied, our synthesis is an environmental-friendly, low-cost, scalable and facile fabrication process.

The morphology and microstructure of Fe2-Z8-C were characterized by SEM, transmission electron microscopy (TEM), scanning transmission electron microscopy (STEM) and Raman spectrum. Figures 2a and S2 show the amorphous structure of Fe2-Z8-C particles with sub-micron sizes. The mapping images in Figure 2b indicate that C, N and Fe elements uniformly distribute over the entire particles. Furthermore, Fe atoms were observed by the high angle annular dark-field STEM (HAADF-STEM) at atomic resolution. As shown in Figures 2c and S3, the high density of Fe single-atoms (highlighted by red circles) on the carbon substrate implies the densely and atomically dispersed Fe-N_x moieties, whose structure will be identified latter. As expected for the carbonized ZIF-8 material, the obtained Fe2-Z8-C possesses a highly microporous structure with high Brunauer-Emmett-Teller (BET) surface area of 1265 m^2 g^{-1} (Figure S4), which are favorable for hosting numerous Fe-N_x active moieties that are essential for the high activity and power density of Fe2-Z8-C in PEMFCs. The local and electronic structure of iron atoms in Fe2-Z8-C were further investigated by X-ray absorption near-edge structure (XANES) and extended X-ray absorption fine structure (EXAFS). The XANES spectra of Fe K-edge in Figure 2d show the similarity of pre-edge characteristic between Fe2-Z8-C and iron phthalocyanine (FePc) spectra which display a fingerprint peak at 7115 eV corresponding to the Fe-N_4 porphyrin plane. Meanwhile the large difference between Fe2-Z8-C and Fe foil spectra further confirms the absence of Fe NPs in Fe2-Z8-C catalyst. As shown in Figure 2e, the Fourier transformed EXAFS spectrum (without phase correction) of Fe2-Z8-C exhibits a sole peak at ~1.6 Å assigning to the Fe-N scattering paths, whereas the Fe-Fe and Fe-C peaks were not detected.[3b, 11b] Although EXAFS spectrum cannot clearly distinguish Fe-N and Fe-O bonds,[13] the existence of iron oxides was less possible since Fe2-Z8 did not contain oxygen element and the annealing was conducted under the inert atmosphere. The EXAFS data were further fitted in *r*-space and *k*-space as shown in Figure S5, and the fitting parameters were summarized in Table S1. It indicates that the isolated Fe atom was four-fold coordinated by N atoms. Meanwhile one O_2 molecule might be adsorbed on the Fe atom in perpendicular to Fe-N_4 plane as shown in the inset of Figure 2d. So, all above structural

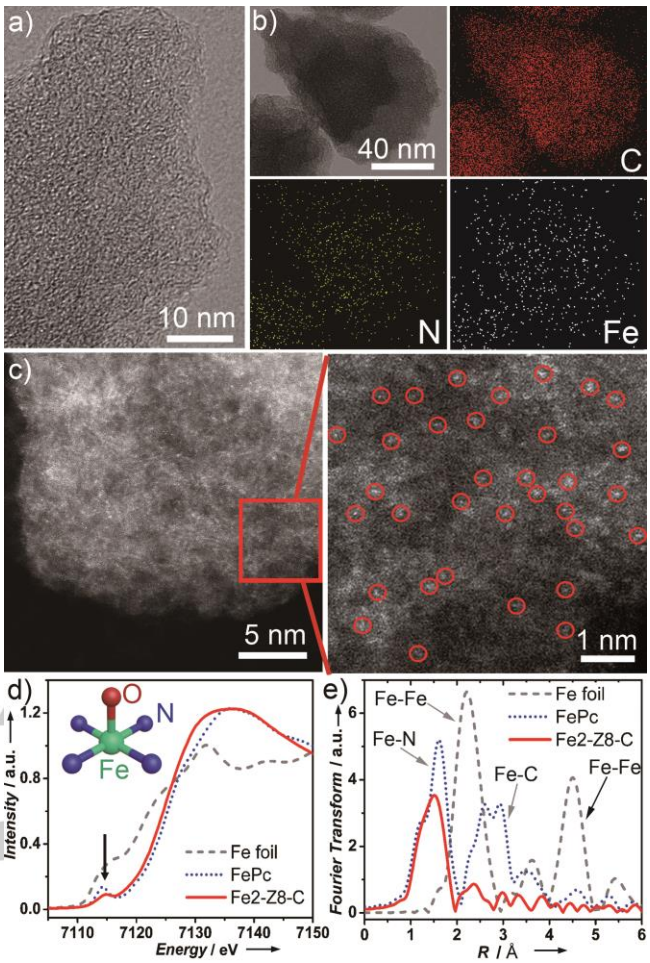

Figure 2. Images and spectra characterizations of Fe2-Z8-C. (a) HRTEM image, (b) STEM images and corresponding elemental mapping, (c) HAADF-STEM images, (d) normalized XANES at Fe K-edge, (e) Fourier-transformed EXAFS of Fe2-Z8-C with references.

characterizations prove that the incorporated Fe(II) dopants were completely converted into atomically dispersed Fe-N_4 moieties in Fe2-Z8-C with no Fe/Fe_3C NPs.

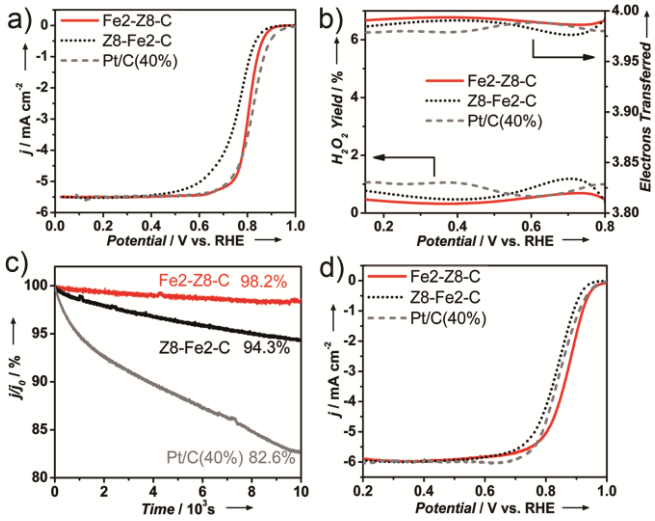

Figure 3. a) LSV curves, b) H_2O_2 yield and electron transfer number and c) normalized i-t cures at 0.5 V (vs. RHE) of Fe2-Z8-C, Z8-Fe2-C, Pt/C(40%) in 0.5 M H_2SO4 by RRDE tests. (d) LSV curves tested in 0.1 M KOH electrolytes. Tests were performed in O_2-saturated electrolytes at 1600 rpm with scan rate of 10 mV s^{-1}. The ring potential was set at 1.25 V vs. RHE.

For comparison, a control sample of Z8-Fe2-C was prepared by physically mixing ZIF-8 with FeOx as the precursor (see Supporting Information for the preparation and characterizations). As shown in Figure S6, Fe NPs formed during pyrolysis, and further catalyzed the growth of CNTs and the graphitization of carbon. According to XPS results, not only the total N content but also the pyridinic N/Fe-N_4 ratio on Fe2-Z8-C surface was higher than those on Z8-Fe2-C surface (Figure S7). It thus further demonstrates that the Fe-N coordination structure in Fe2-Z8 successfully isolated Fe from agglomeration and produced more Fe-N_4 moieties compared with the mixture of FeOx/ZIF-8.

The ORR activities of the catalysts were firstly evaluated by the rotating ring-disk electrode (RRDE) technique. The linear sweep voltammetry (LSV) curve in Figure 3a shows the excellent activity of Fe2-Z8-C with a high onset potential (E_{onset}) of 0.902 V (defined as the potential with a current density of 0.1 mA cm^{-2}) and a half-wave potential ($E_{1/2}$) of 0.805 V in 0.5 M H_2SO_4, which is comparable to the commercial Pt/C ($E_{1/2}$: 0.822 V) and among the top level NPMCs. The low H_2O_2 yield (below 1%) and the close-to-four electron transfer number demonstrate a high selectivity of 4 e^- oxygen reduction reaction for Fe2-Z8-C (Figure 3b). Furthermore, the durability of Fe2-Z8-C was evaluated in an O_2-saturated acid electrolyte by the chronoamperometric test model at a constant potential of 0.5 V. Figure 3c shows a 98.2% current retention for the Fe2-Z8-C after 10 k seconds, significantly higher than 82.6% of Pt/C and 94.3% of Z8-Fe2-C. The LSV curve of Fe2-Z8-C after the chronoamperometric test shows a 17 mV decrease of $E_{1/2}$, less than the 38 mV of Z8-Fe2-C (Figure S8). Additionally, the electrochemical activities of the as-prepared catalysts were evaluated in 0.1 M KOH electrolyte. As presented in Figure 3d, Fe2-Z8-C processes an E_{onset} of 0.985 V and an $E_{1/2}$ of 0.871 V, considerably higher than those of Pt/C (0.974 V and 0.847 V respectively).

The strong adsorption of SCN^- to Fe ions could impede the absorption of O_2 onto Fe-N_4 sites and thus block the ORR on these sites. Based on this phenomenon, a poisoning experiment was performed by adding 0.01 M KSCN into the electrolyte during the ORR test. A dramatic negative shift of half-wave potential (56 mV) on LSV curves was observed (Figure S9), which proved the high ORR activity of Fe2-Z8-C could be ascribed to the Fe-N_4 moieties. As discussed above, doping Fe(II) into ZIF-8 ensured atomically dispersed and fixed Fe ions in the precursor, which could be completely converted into Fe-N_4 moieties during the pyrolysis when the Fe ion concentration was below a threshold as will be discussed latter. It is believed that the higher content of Fe-N_4 active moieties on Fe2-Z8-C endows its superior ORR properties to the Fe NPs-existed Z8-Fe2-C.

To further demonstrate the compositional and structural advantages of densely distributed Fe-N_4 active moieties in the actual fuel cell working condition, Fe2-Z8-C was assembled in a 5 cm^2 PEMFC as the cathode catalyst. Under absolute H_2/O_2 pressures of 2.5 bar and a catalyst loading of 2.8 mg cm^{-2}, high PEMFC activities and power densities were achieved with the

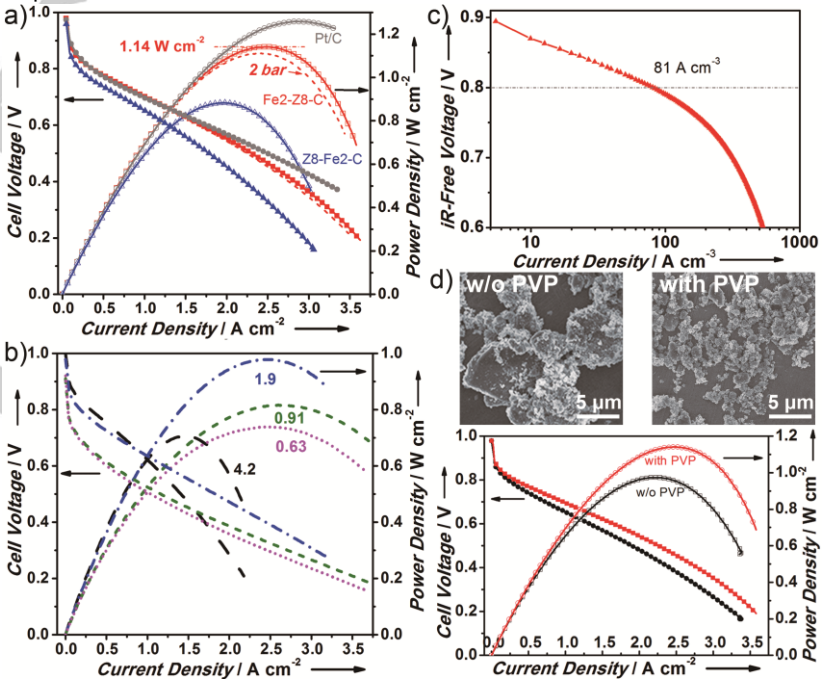

Figure 4. I-V polarization and power density curves of a) Fe2-Z8-C, Z8-Fe2-C, and Pt/C(20%) with cathode loadings of 2.8, 2.7 and 0.33 (Pt) mg cm^{-2} respectively; and b) Fe2-Z8-C with indicated loadings; c) Tafel plot of Fe2-Z8-C (1.9 mg cm^{-2}) measured under DOE(U.S.) stand: 1 bar; d) comparison between Fe2-Z8-C (2.8 mg cm^{-2}) with or without applying PVP coating before the carbonization of Fe2-Z8. PEMFC tests were applied in a 5 cm^2 single cell with 80 °C H_2/O_2 at flow of 0.3 L min^{-1} for H_2 and 0.4 L min^{-1} for O_2, 100%RH, 2.5 bar absolute pressure (except specifically indicated). Membrane: NRE 211.

current densities of 35, 310, and 1650 mA cm^{-2} at the potential of 0.9, 0.8, and 0.6 V, respectively (Figure 4a), which are the top performances among NPMC-derived PEMFCs, see Table S2. Besides, we noticed that the polarization curves of Fe2-Z8-C overlapped that of Pt/C(20%) from the open circuit voltage (OCV) till 0.6 V, indicating a high PEMFC activity of Fe2-Z8-C due to its high active-moiety density. More significantly, the P_{max} reached 1141 mW cm^{-2}, and it only slightly decreased to 1110 mW cm^{-2} when the fuel pressure was reduced to 2 bar. These extremely high power densities outperformed all reported NPMCs measured under similar condition to the best of our knowledge. In contrast, Z8-Fe2-C displayed relatively poor PEMFC performances on both power density (P_{max} = 880 mW cm^{-2}) and current density (150 mA cm^{-2}@0.8 V) due to the waste of Fe precursor and the reduction of active sites as demonstrated above.

Interestingly, Figure 4b shows that the high P_{max} could be obtained within a wide range of Fe2-Z8-C loading, e.g. 1000 and 810 mW cm^{-2} for 1.9 and 0.91 mg cm^{-2}, respectively. Even with a very low loading of 0.63 mg cm^{-2}, the PEMFC still achieved a remarkably high P_{max} of 740 mW cm^{-2}. This phenomenon should be attributed to the densely dispersed Fe-N_4 moieties on Fe2-Z8-C, which supplied sufficient activity at a thin catalyst layer. Different from most previously reported NPMCs, whose P_{max} were usually obtained at a high loading near 4 mg cm^{-2},[4c, d, 14] the Fe2-Z8-C achieved the best power performance with 2~3 mg cm^{-2} catalysts. A high Fe2-Z8-C loading of 4.2 mg cm^{-2} generated a relatively low power density due to the large thickness-induced high internal resistance (Figure S10), which caused a fast voltage decay with the increased current. In addition to the power density, the volumetric current density at 0.8 $V_{iR\text{-}Free}$ is another crucial parameter for judging the catalytic activity of NPMCs. Because of the densely dispersed Fe-N_4 active moieties over the high surface area microporous carbon support, the Fe2-Z8-C delivered a high volumetric current density of 81 A cm^{-3}@0.8$V_{iR\text{-}Free}$ under U.S. DOE standard at the loading of 1.9 mg cm^{-2} (Figure 4c, Figure S11).

It is worth mentioning that the PVP coating plays an important role for Fe2-Z8-C to achieve the high PEMFC performance. When the Fe2-Z8 was dipped in a dilute PVP solution, a molecular layer of PVP was adsorbed on Fe2-Z8 surface (see Figure S12). The PVP coating could prevent the fusion of Fe2-Z8 crystals because PVP was decomposed from 400 to 480 °C, while Fe2-Z8 already started to decompose around 510 °C (Figure S13). Therefore, PVP coating could prohibit the formation of large catalyst particles thus ensuring the large surface utilization. In Figure 4d, it is seen that the Fe2-Z8-C particles without PVP coating had a rather wide size distribution with several-micron large particles. (See Figure S14 for more image information) In contrast, PVP coating resulted in smaller and more uniform Fe2-Z8-C NPs with a higher surface area and more micropores (Figure S15). Correspondingly, the Fe2-Z8-C with PVP coating-treatment showed higher power and current densities than its counterpart in PEMFCs. Interestingly, the RDE results given in Figure S16, show the same E_{onset} and $E_{1/2}$ for Fe2-Z8-C with or without PVP coating on the precursor Fe2-Z8. The non-consistent results by RDE and PEMFC techniques suggest the measured results by the three-electrode system (half-cell) may be not sufficient to predict the performance of NPMCs in a real PEMFC, and meanwhile emphasize the crucial role of PEMFC characterization of NPMCs for evaluating their practical application potential.

The optimal iron content in the doped ZIF-8 was explored by a series of characterizations of XRD, SEM, TEM, and RRDE. At a low doping level ($x \leq 2$), the crystallinity of Fex-Z8 was improved and the brown color became darker with increasing Fe content (Figure S17a-c). Whereas excessive amounts of Fe dopants would lighten the crystal color and change the crystal phase as proved by the appearance of new diffraction peaks for Fe5-Z8. Although the new diffraction peaks did not appear in Fe3.5-Z8 (Figure S17j), Fe NPs were found in Fe3.5-Z8-C as shown in Figure S18c, d, suggesting Fe atoms began to agglomerate at this density. Thus, 2 mole percent of Fe was chosen to be the optimal doping level in our experiment, which led to 3 wt.% atomically dispersed Fe atoms in Fe2-Z8-C as determined by the XPS measurement (Figure S19). In Figure S20, electrochemical tests proved that the catalyst with atomically dispersed Fe atoms was an ideal structure to achieve the highest catalytic activity. Despite the comparable activity of Fe3.5-Z8-C to Fe2-Z8-C in the acid, the relatively weak durability of Fe3.5-Z8-C (see Figure S20c) implies again that the formation of Fe nanoparticles could decrease the stability of the catalyst in the three-electrode system. In addition, the extension of annealing duration from 1 hour to 2 hours promoted the ORR activity because of the increased micropores and BET surface area (Figure S21).

In summary, this work developed a facile, low cost, environmental-friendly and scalable solid-synthesis method for a highly active Fe-N-C electrocatalyst with Fe exclusively in Fe-N_4 moieties. The as-prepared Fe2-Z8-C delivered the highest current density of 1.65 A cm^{-2} at 0.6 V, and an unprecedented power density of 1.14 W cm^{-2} in acidic PEMFCs. Even with low catalyst loadings of 1.9 and 0.9 mg cm^{-2}, its power density still achieved 1.00 and 0.81 W cm^{-2} respectively. The densely and atomically dispersed Fe-N_4 active moieties as well as the uniform and small catalyst nanoparticles were essential for the excellent PEMFC performance. This work makes a step forward toward the better fabrication of highly pure and active NPMCs for PEMFC applications.

Acknowledgements

This work was supported by the National Natural Science Foundation of China (Grant No.21673014), and the “111“ Project (B17002) funded by the Ministry of Education of China.

Keywords: Electrocatalysis; PEM fuel cell; Fe-N-C; Oxygen reduction; Solid-phase synthesis

[1] a) M. K. Debe, *Nature* **2012**, *486*, 43–51; b) M. Shao, Q. Chang, J.-P. Dodelet, R. Chenitz, *Chem. Rev.* **2016**, *116*, 3594–3657; c) F. Jaouen, E. Proietti, M. Lefèvre, R. Chenitz, J. P. Dodelet, G. Wu, H. T. Chung, C. M. Johnston, P. Zelenay, *Energy Environ. Sci.* **2011**, *4*, 114–130; d) V. Armel, S. Hindocha, F. Salles, S. Bennett, D. Jones, F. Jaouen, *J. Am. Chem. Soc.* **2017**, *139*, 453–464.

[2] a) H. A. Gasteiger, N. M. Marković, *Science* **2009**, *324*, 48–49; b) C. Tang, Q. Zhang, *Adv. Mater.* **2017**, *29*, 1604103; c) Y. Liu, X. Yue, K. Li, J. Qiao, D. P. Wilkinson, J. Zhang, *Coordin. Chem. Rev.* **2016**, *315*, 153–177; d) D. He, H. Tang, Z. Kou, M. Pan, X. Sun, J. Zhang, S. Mu,

Adv. Mater. **2017**, *29*, 1601741; e) Z. Song, N. Cheng, A. Lushington, X. Sun, *Catalysts* **2016**, *6*, 116.

[3] a) W. Zhang, W. Lai, R. Cao, *Chem. Rev.* **2017**, *117*, 3717–3797; b) Q. Jia, N. Ramaswamy, U. Tylus, K. Strickland, J. Li, A. Serov, K. Artyushkova, P. Atanassov, J. Anibal, C. Gumeci, S. C. Barton, M.-T. Sougrati, F. Jaouen, B. Halevi, S. Mukerjee, *Nano Energy* **2016**, *29*, 65–82; c) X. Zeng, J. Shui, X. Liu, Q. Liu, Y. Li, J. Shang, L. Zheng, R. Yu, *Adv. Energy Mater.* **2017**, 1701345.

[4] a) E. Proietti, F. Jaouen, M. Lefèvre, N. Larouche, J. Tian, J. Herranz, J.-P. Dodelet, *Nat. Commun.* **2011**, *2*, 416; b) J. Shui, C. Chen, L. Grabstanowicz, D. Zhao, D.-J. Liu, *Proc. Natl. Acad. Sci.* **2015**, *112*, 10629–10634; c) Y.-C. Wang, Y.-J. Lai, L. Song, Z.-Y. Zhou, J.-G. Liu, Q. Wang, X.-D. Yang, C. Chen, W. Shi, Y.-P. Zheng, M. Rauf, S.-G. Sun, *Angew. Chem. Int. Ed.* **2015**, *54*, 9907–9910; d) X. Fu, P. Zamani, J. Y. Choi, F. M. Hassan, G. Jiang, D. C. Higgins, Y. Zhang, M. A. Hoque, Z. Chen, *Adv. Mater.* **2017**, *29*, 1604456.

[5] a) C. Zhang, Y. C. Wang, B. An, R. Huang, C. Wang, Z. Zhou, W. Lin, *Adv. Mater.* **2017**, *29*, 1604556; b) W. J. Jiang, L. Gu, L. Li, Y. Zhang, X. Zhang, L. J. Zhang, J. Q. Wang, J. S. Hu, Z. Wei, L. J. Wan, *J. Am. Chem. Soc.* **2016**, *138*, 3570–3578.

[6] C. Zhu, H. Li, S. Fu, D. Du, Y. Lin, *Chem. Soc. Rev.* **2016**, *45*, 517–531.

[7] M. Zhou, H.-L. Wang, S. Guo, *Chem. Soc. Rev.* **2016**, *45*, 1273–1307.

[8] a) F. Jaouen, J. Herranz, M. Lefèvre, J.-P. Dodelet, U. I. Kramm, I. Herrmann, P. Bogdanoff, J. Maruyama, T. Nagaoka, A. Garsuch, J. R. Dahn, T. Olson, S. Pylypenko, P. Atanassov, E. A. Ustinov, *ACS Appl. Mater. Interfaces* **2009**, *1*, 1623–1639; b) M. Lefèvre, E. Proietti, F. Jaouen, J.-P. Dodelet, *Science* **2009**, *324*, 71–74; c) G. Wu, K. L. More, C. M. Johnston, P. Zelenay, *Science* **2011**, *332*, 443–447; d) Z. Y. Wu, X. X. Xu, B. C. Hu, H. W. Liang, Y. Lin, L. F. Chen, S. H. Yu, *Angew. Chem. Int. Ed.* **2015**, *54*, 8179–8183; e) S. H. Ahn, X. Yu, A. Manthiram, *Adv. Mater.* **2017**, 1606534.

[9] a) M. Ferrandon, A. J. Kropf, D. J. Myers, K. Artyushkova, U. Kramm, P. Bogdanoff, G. Wu, C. M. Johnston, P. Zelenay, *J. Phys. Chem. C* **2012**, *116*, 16001–16013; b) W. Liu, L. Zhang, W. Yan, X. Liu, X. Yang, S. Miao, W. Wang, A. Wang, T. Zhang, *Chem. Sci.* **2016**, *7*, 5758–5764; c) P. Yin, T. Yao, Y. Wu, L. Zheng, Y. Lin, W. Liu, H. Ju, J. Zhu, X. Hong, Z. Deng, G. Zhou, S. Wei, Y. Li, *Angew. Chem. Int. Ed.* **2016**, *55*, 10800–10805.

[10] a) D. Zhao, J. L. Shui, L. R. Grabstanowicz, C. Chen, S. M. Commet, T. Xu, J. Lu, D. J. Liu, *Adv. Mater.* **2014**, *26*, 1093–1097; b) J. Li, Y. Song, G. Zhang, H. Liu, Y. Wang, S. Sun, X. Guo, *Adv. Funct. Mater.* **2017**, *27*, 1604356.

[11] a) H. Meng, N. Larouche, M. Lefèvre, F. Jaouen, B. Stansfield, J.-P. Dodelet, *Electrochim. Acta* **2010**, *55*, 6450–6461; b) A. Zitolo, V. Goellner, V. Armel, M.-T. Sougrati, T. Mineva, L. Stievano, E. Fonda, F. Jaouen, *Nat. Mater.* **2015**, *14*, 937–942; c) H. Shen, E. Gracia-Espino, J. Ma, H. Tang, X. Mamat, T. Wagberg, G. Hu, S. Guo, *Nano Energy* **2017**, *35*, 9–16.

[12] X. J. Wang, H. G. Zhang, H. H. Lin, S. Gupta, C. Wang, Z. X. Tao, H. Fu, T. Wang, J. Zheng, G. Wu, X. G. Li, *Nano Energy* **2016**, *25*, 110–119.

[13] Y. Chen, S. Ji, Y. Wang, J. Dong, W. Chen, Z. Li, R. Shen, L. Zheng, Z. Zhuang, D. Wang, Y. Li, *Angew. Chem. Int. Ed.* **2017**, *56*, 6937–6941.

[14] Y. Yao, Y. You, G. Zhang, J. Liu, H. Sun, Z. Zou, S. Sun, *ACS Appl. Mater. Interfaces* **2016**, *8*, 6464–6471.

10.1002/anie.201709597

WILEY-VCH

Table of Contents

COMMUNICATION

An environmental-friendly, facile, low cost, and scalable solid-synthesis method was developed for a highly active Fe-N-C electrocatalyst with Fe exclusively in Fe-N_4 moieties. The as-prepared Fe2-Z8-C delivered an unprecedented power density of 1.14 W cm^{-2} in the acidic PEMFC, which was attributed to the densely and atomically dispersed Fe-N_4 active moieties, and the small catalyst nanoparticles.

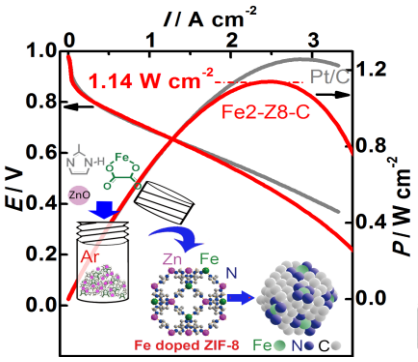

Qingtao Liu, Xiaofang Liu, Lirong Zheng, and Jianglan Shui**

Page No. – Page No.

Environmental-Friendly Solid Synthesis of Fe-N-C Electrocatalyst with Fe Exclusively in Atomically Dispersed Fe-N_4 Moieties for High-Power Proton Exchange Membrane Fuel Cells